Cyclic behaviour of as-built and strengthened existing reinforced concrete columns previously damaged by fire

José Melo[1*], Zafiris Triantafyllidis[2], David Rush[3], Luke Bisby[3], Tiziana Rossetto[4], António Arêde[1], Humberto Varum[1], Ioanna Ioannou[4]

[1] CONSTRUCT-LESE, Faculty of Engineering (FEUP), University of Porto, Porto, Portugal
[2] Empa, Swiss Federal Laboratories for Materials Science and Technology, Dübendorf, Switzerland
[3] Edinburgh Fire Research Centre, School of Engineering, University of Edinburgh, Edinburgh, UK
[4] EPICentre, University College London, London, UK
[*] Corresponding Author: josemelo@fe.up.pt

Abstract

A structure, during its life, may be subjected to multiple hazards. These hazards are sometimes combined over a short period of time, or in some cases occur many years apart, with the first hazard influencing the structural response under a second hazard. A reinforced concrete (RC) structure previously damaged by fire and then exposed to seismic loading is one such example. To assess such structures, the effects of fire on the cyclic performance of RC elements needs to be better understood. Moreover, it is also important to develop and validate strengthening methods that can reinstate or improve the seismic performance of fire-damaged RC elements. This paper presents the results of a novel experimental campaign where six full-scale RC columns with detailing representing existing Mediterranean buildings designed to old seismic codes are subjected to fire and then cyclic loading. Four RC columns were damaged after exposure to 30 or 90 minutes of the ISO 834 standard fire curve in a furnace and then tested under uniaxial cyclic lateral loading up to failure. Two of these columns were repaired and strengthened post-fire with Carbon Fibre Reinforced Polymer (CFRP) wrapping. The strengthening method aimed to increase the concrete strength through confinement, and to increase the displacement ductility and energy dissipation capacity under seismic loading. Two additional control columns, one as-built and another strengthened, were cyclically tested for comparison with the fire-damaged columns. It was found that the 30 minute fire exposure resulted in few concrete cracks, whilst cover spalling and general cracking was observed in the 90 minute fire exposure. A significant decrease in the displacement ductility and dissipated energy of the columns was observed following fire exposure, even for the 30 minute fire. The columns that had post-fire

repair and CFRP strengthening, showed better cyclic performance than the control column without fire exposure. It was also found that post-fire strengthened columns may reach similar seismic performance than similarly strengthened columns without previous fire damage.

Keywords: Existing RC columns, fire damage, post-fire strengthening, post-fire cyclic loading, experimental tests

1. Introduction

1.1. Background

Reinforced concrete (RC) structures are widely perceived to perform well in fires owing to the incombustibility and relatively low thermal conductivity of concrete, as well as the high thermal massivity of typical RC sections [1, 2]. Although historically there have been several catastrophic failures during fire (or immediately after fire/upon cooling), it is generally accepted in engineering practice that, in most cases, concrete structures can be repaired and brought back to service [1, 3]. Despite this fact, structural design for fire was performed for many decades predominantly based on fulfilling life safety and fire spread prevention objectives in a prescriptive framework of assigning (or providing) 'fire resistance' to structural elements, without explicit consideration of property protection design objectives. Performance-based approaches that would enable the design for defined structural performance criteria and property protection (and hence, repairability and service continuation after a fire) were only introduced in codes relatively recently [4, 5]; however, their implementation is still not wide in practice for concrete structures [6]. Although material behaviour has been studied fairly well (for example, fib Bulletin 46 [2] provides a review of both high temperature and residual properties) as well as the behaviour of isolated RC elements under standard fire exposure during many decades of fire resistance testing, there are still knowledge gaps regarding the structural behaviour of RC structures in real fires, their post-fire behaviour during cooling, and their residual capacity, amongst others [6, 7]. These are critical for assessing the condition of a fire-

exposed RC structure and establishing efficient repair and retrofitting strategies, particularly since repairability, rapid reoccupation and structural resilience against multiple hazards become nowadays increasingly important [8].

Existing guidelines [2, 3] for evaluating damage and the post-fire residual capacity are mostly focusing on qualitative and empirical assessments, and structural analysis based on non- and partially destructive testing of the fire-exposed structural elements. Recent efforts were also made towards the development of intensity measures, damage indices, and quantifiable damage consequences for probabilistic performance- and reliability-based assessments [9-11]. However, the latter are still a very active field of research and the respective framework for fire is not yet as well-established as in other fields, e.g. seismic engineering. Performance-based approaches on the other hand are implemented in seismic design codes (e.g. [12, 13]), and more importantly they are implemented in the assessment and retrofit of existing buildings, since older structures that were not designed to current codes and construction practices often require explicit verification of their seismic vulnerability [14]. With regards to the combined hazard of earthquake and fire, there have been several studies addressing the fire response of structures previously damaged by earthquake [15-18]. However, earthquake is also a credible hazard for the remaining lifespan of structures in seismic zones that may be repaired and reused after an accidental fire event. Currently there is no design guidance in this direction and only few experimental [19-23] and numerical [24-26] studies are available regarding the seismic/cyclic performance of fire-exposed RC structures.

1.2. Residual cyclic behaviour of columns after fire exposure

This paper focuses on the post-fire cyclic behaviour and retrofit of columns, which are critical elements for preventing the formation of soft-storey collapse mechanisms in RC-framed buildings during earthquake [14]. Early experimental results from columns tested under standard fire exposure followed by a cooling stage [27] indicated that temperature continues to increase significantly in the concrete core for a substantial duration after cooling has begun. In a numerical parametric study of axially loaded columns exposed to natural (parametric) fires, Dimia et al. [28] showed that due to this

delayed/prolonged temperature rise within the core and the additional concrete strength degradation that occurs during cooling, collapse is even likely to occur in certain cases several hours after the compartment temperature has cooled down to ambient. Although the actual post-fire capacity mainly depends on fire severity, the geometric characteristics of the column (thermal massivity and slenderness), and the load level during fire [28, 29], previous studies on columns that have cooled down to ambient after standard fire testing showed significant reductions regarding both the axial load capacity [30, 31] and the lateral/flexural strength and stiffness [25, 32].

With respect to the cyclic/seismic performance, the study by Ni and Birely [26] on the post-fire response of flexure-controlled RC walls corroborates the above findings regarding strength and stiffness degradation, and in addition it shows that the failure drift of the walls reduces for standard fire durations greater than 60 minutes. An experimental study by Li et al. [21] on high performance concrete frames that were subjected to 140 minutes of the ISO 834 standard fire [33] shows that fire damage resulted in significant pinching behaviour under cyclic loading compared to the corresponding unheated frames. Higher stiffness degradation and considerably lower ductility and dissipated energy were also observed in the fire-exposed frames. Demir et al. investigated the residual cyclic behaviour of flexure-critical columns made of normal strength concrete [22] and recycled aggregate concrete [34] after exposure to 30, 60 and 90 minutes of the ISO 834 standard fire. They also observed increasing reductions in the lateral load capacity, flexural stiffness and energy dissipation capacity of the columns with increasing fire durations, although the ductility factors were in all cases greater than 3.5 and considered satisfactory. Furthermore, they observed that a larger concrete cover depth has an adverse effect on the stiffness (and subsequently, the yield displacement and ductility) of the column, whereas it does not have a significant impact on the lateral load and energy dissipation capacity [22]. In [35], Demir et al. also considered the effect of ageing after fire exposure on the cyclic performance of columns to investigate the influence of the known long-term (partial) strength recovery of concrete [36]; however, they did not observe any significant differences between columns tested at 30 and 60 days after fire exposure, whereas no conclusions could be drawn from testing at 360 days of ageing due to experimental problems. Nonetheless, as Mostafaei et al.

[25] point out, despite the fact that concrete exposed to 500ºC may gain up to 90% of its original compressive strength one year after fire, the risk of an earthquake occurring soon after the column has been exposed to fire cannot be neglected and this strength recovery cannot be relied upon.

1.3. Current repair strategies and aims of the current work

Traditional repair techniques involve the replacement of the overheated zone near the exposed concrete surface (often the concrete cover), such that it continues to provide thermal protection to the rebar and inner concrete core, or the enlargement of the concrete section using cast or sprayed concrete [1, 3]. From the above discussion it becomes apparent that repairing a column "superficially" by cover reinstatement may not be sufficient for seismic resistance, since the concrete core can also deteriorate in natural fires due the propagating "thermal wave" during and after the decay phase of the fire, whereas cross-section enlargement can potentially be detrimental to the global structural response by affecting load paths and load redistribution during an earthquake. Furthermore, none of the reviewed studies above look at potential repair and retrofitting solutions that could improve the seismic performance of the RC elements previously damaged by fire.

This paper considers fibre-reinforced polymer (FRP) wrapping in combination with concrete cover replacement as an efficient and rapid repair/retrofit strategy for fire exposed columns. Although nowadays FRP wrapping is widely used in column strengthening and seismic retrofit, previous research on strengthening fire-damaged concrete appears to be rather scarce. Previous studies showed that FRP wraps are very effective in increasing the compressive strength of plain concrete cylinders [37, 38] as well as the axial capacity of small-scale reinforced columns [39, 40], which were previously exposed to elevated temperature. Furthermore, Yaqub & Bailey [41] investigated the cyclic performance of small-scale, shear-critical columns that had been previously heated up to a uniform temperature of 500ºC and strengthened by FRP wrapping. However, to the authors' best knowledge there is no previous study regarding the effectiveness of FRP wraps in strengthening full-scale columns for lateral cyclic loading, which have previously suffered damage from realistic fire exposures.

This paper aims to investigate experimentally the cyclic response in lateral loading of (i) fire-damaged RC columns and (ii) post-fire repaired and FRP-strengthened RC columns, which were previously damaged by exposure to two well-defined, representative fire severities. These are realised by exposing the columns to the ISO 834 standard time-temperature curve followed by a decay phase, thus resembling to two realistic scenarios (of the many possible) that could be encountered in a real building fire. A standard fire testing framework is adopted herein such that fire damage and residual cyclic response are characterised under well-defined conditions, and that the obtained experimental data can be used as input in fragility curve development studies (such as [10]), whereas it is anticipated that this will be complemented in the future with similar test campaigns in a representative spectrum of natural/parametric (and real) fires. The repair and FRP strengthening techniques examined herein aim to reduce the post-fire seismic vulnerability of existing RC buildings which are typical in the Mediterranean region, by increasing the heat-affected concrete strength, the ductility and energy dissipation capacity of RC columns through external confinement.

2. Experimental Procedure

2.1. Test programme

The experimental campaign consisted of six full-scale RC columns and was divided into three phases, namely: i) fire exposure; ii) repair and strengthening of the columns; iii) lateral cyclic loading test with constant axial load until failure. Fire exposure was realised by means of standard fire testing in a furnace, for two different durations of the ISO 834 time-temperature curve [42], denoted herein as 'medium' (30 min) and 'long' (90 min) for the purposes of the discussion that follows below. Two columns (M and M-S) were exposed to the medium fire duration and one column was later repaired and strengthened (M-S). Two more columns (L and L-S) were tested under the longer fire duration and then one of them was repaired and strengthened (L-S). The four specimens tested under fire conditions were subsequently tested under lateral cyclic loading. Two control columns were also cast that were not exposed to fire and were only tested under lateral cyclic loading. Both control specimens had the same geometry and detailing as the other columns, with one being unstrengthened (C) and

the other being strengthened with CFRP wrapping (C-S). The fire exposure, repair and testing conditions for each specimen are summarised in Table 1.

Table 1 – Specimens ID and corresponding fire exposure and repair and strengthening scheme.

Specimen ID	Fire Exposure	Repair & strengthening scheme	Cyclic Testing
C	–	–	Yes
C-S	–	CFRP wrapping	Yes
M	30 min	–	Yes
M-S	30 min	Cover reinstatement and CFRP wrapping	Yes
L	90 min	–	Yes
L-S	90 min	Cover reinstatement and CFRP wrapping	Yes

2.2. Specimen detailing and material properties

All column specimens had identical square cross-sections and reinforcement detailing. The specimens were designed according to an old Portuguese code [43] and consequently without seismic and fire requirements. This code is representative of RC building design in Mediterranean countries in the 1950s-1970s, and each specimen represents a half-storey cantilever column of a 3.0 m storey height, at foundation level, of a structure with three or four storeys. Therefore, the lateral load was applied at a level of 1.5 m from the top foundation, but the column specimens had an additional 0.15 m length (1.65 m) to enable them to be attached to the lateral actuator. The geometry and cross-section details are presented in Figure 1. The columns had a square cross-section with dimensions 0.30×0.30 m^2, and the foundation consisted of a stiff block with dimensions $0.44 \times 0.44 \times 0.5$ m^3. The columns have eight 12 mm diameter longitudinal reinforcing bars (longitudinal reinforcement ratio of 1%) and stirrups of 6 mm diameter spaced at 0.15 m centres and having 90° anchorage hooks. The concrete cover was 25 mm, whereas the concrete mix contained crushed limestone aggregates with a maximum size of 25 mm. The specimens were all cast at the same time and cured for at least 6 months at ambient laboratory temperature and relative humidity conditions, to reduce the risk of explosive spalling during furnace testing.

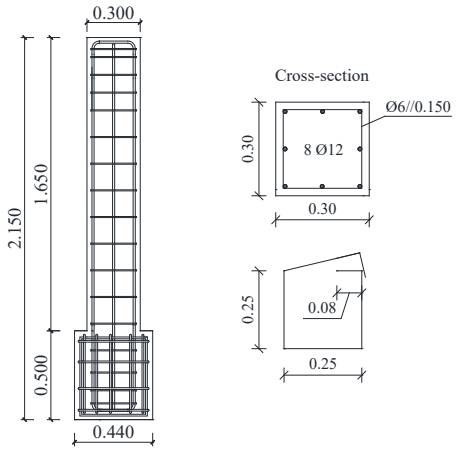

a) b)

Figure 1 – Geometry and reinforcement detailing: a) global dimensions; b) cross-section (dimensions in m).

Table 2 summarises the mean values of the concrete and steel properties, where f_{cm} is the concrete compressive strength of cylinder samples (Ø150mm × 300mm), f_{ym} is the yield strength of reinforcement, f_{um} is the ultimate tensile strength of reinforcement and ε_{cu} is the ultimate strain of reinforcement. The concrete cylinder samples were tested according to the standard norm NP EN 206-1 [44], after 6 months of curing and when the first cyclic test was performed on the control specimen (C).

Table 2 – Mean values of the concrete and steel mechanical properties.

Material	Mechanical property	
Concrete	f_{cm} (MPa)	33.5
Steel - Ø12mm	f_{ym} (MPa)	445
	f_{um} (MPa)	571
	ε_{cu} (%)	17.5
Steel - Ø6mm	f_{ym} (MPa)	540
	f_{um} (MPa)	639
	ε_{cu} (%)	18

2.3. Fire exposure setup

The fire tests were performed using a vertical furnace with internal dimensions of 3.1 × 3.1 × 1.2 m^3 (h × w × d) located at the Structural and Fire Resistance Laboratory at Aveiro University, Portugal. The furnace can perform standard fire resistance tests on materials and construction elements according to the European Standards. Propane gas is used to heat the furnace with burner outlets located at the two opposite narrow sides of the furnace. The entire front panel of the furnace is

removable to permit specimens to be placed in and removed from the furnace. Figure 2 shows the front and the lateral views of the furnace.

Each of columns M, M-S, L and L-S was positioned centrally in the furnace and tested individually under the respective fire conditions. All sides of the foundation block and the column top were protected from heat with a 50 mm thick layer of ceramic fibre blanket insulation (density of 128kg/m^3) as presented in Figure 2. This was provided to prevent fire damage (and hence premature failures) on the foundation block and load introduction point at the column top during application of the axial and lateral loads in the cyclic test.

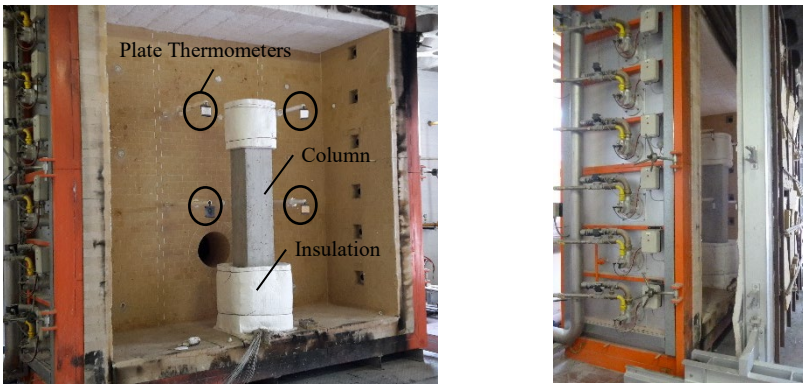

a) b)

Figure 2 – Fire test setup: a) front view; b) lateral view.

The temperature evolution during the fire test followed the ISO 834 [42] standard fire curve for 30 minutes (here designated “medium” fire) in columns M and M-S and 90 minutes (designated “long” fire) in columns L and L-S. Standard fire durations of 30 and 90 minute were selected in order to induce relatively light and severe fire damage to the column specimens in line with the fragility curves developed by [8]. The ISO 834 and the imposed time-temperature curves are presented in Figure 3-a. The control of the furnace temperature was based on the average temperature measured by four plate thermometers (PT) located around the column as shown in Figure 2-a. The peak mean gas phase temperatures measured by PTs at the end of each heating phase were 842°C and 1006°C (standard deviations of ±14ºC and ±8ºC) for the adopted medium and long fires, respectively. After the fire exposures reached the time set point (30 or 90 minutes), the propane burners were turned off and the furnace was allowed to cool naturally. In the cooling phase, the furnace was kept closed until the

interior temperature dropped to at least 100°C. The cooling phase lasted 10 and 24 hours for columns tested under the medium and long fires, respectively.

The temperature of the concrete and reinforcement was monitored by 32 Type-K fiberglass-sheathed thermocouples installed before concrete casting in four sections of the column (AA', BB', CC' and DD' in Figure 3-b). Of these, 11 thermocouples were placed in each column section (AA' and BB') located in the maximum moment region developed during the cyclic tests, and 5 thermocouples in each foundation section (CC' and DD') as shown in Figure 3-b. Thermocouples 2, 6, 9 and 10 of sections AA' and BB' and thermocouples 2 and 4 of sections CC' and DD' were attached on the longitudinal reinforcement. Thermocouples 1&7 and 8&11 were embedded at the centre of the column surface and at the corners, respectively, facing towards the burner outlets at each side of the furnace. The remaining thermocouples were distributed in such a way as to measure a representative temperature profile across the section.

It must be highlighted here that the columns were exposed to fire without any applied load (or restraint) during the furnace test. Thus, the effects of transient thermal creep (or load-induced thermal strain) on the fire behaviour and residual deformation of the columns, which would otherwise be present in a real fire scenario, are not reproduced with this setup. In a real fire, where a column is likely to be subjected to some eccentricity of loading and possibly non-uniform heating (unlike the intentionally controlled and idealised conditions of a standard furnace test), significant residual lateral deflections may remain upon cooling down in a real building. These will be largely due to the irrecoverable deformation of concrete during the heating and cooling stages, and may be relevant for the post-fire structural behaviour since they can alter the load path compared to the non-damaged pre-fire condition, and may also introduce additional second-order effects [45]. Previous research on the fire resistance of reinforced concrete columns with sustained loading has not provided generalised conclusions regarding these effects on the structural behaviour during and after fire [46]. However, recent experimental studies [46] and recent advanced numerical models that can predict the structural response during heating and cooling with reasonable accuracy [47-49] are expected to provide useful insights towards understanding concrete column response in real fires.

Therefore, the effects of residual deflection on a loaded fire-exposed column are not treated in the current paper; these are not considered critical for the purposes of the current study, which focuses on the impact of the irreversible degradation of concrete properties on the post-fire response to lateral cyclic loading. Mechanical degradation from heating of the outermost zones of the cross-section is expected to reduce the radius of gyration of the column's cross-section [29] and thus reduce the lateral load bearing capacity and stiffness of the column under earthquake loading. However, the possible additional second-order effects on the seismic behaviour of the column, which may be caused by residual post-fire deflections, should be addressed in future experimental campaigns on columns exposed to real fires, as suggested previously in Section 2.3, and ought to be considered by designers seeking to implement the strengthening technique presented in this paper.

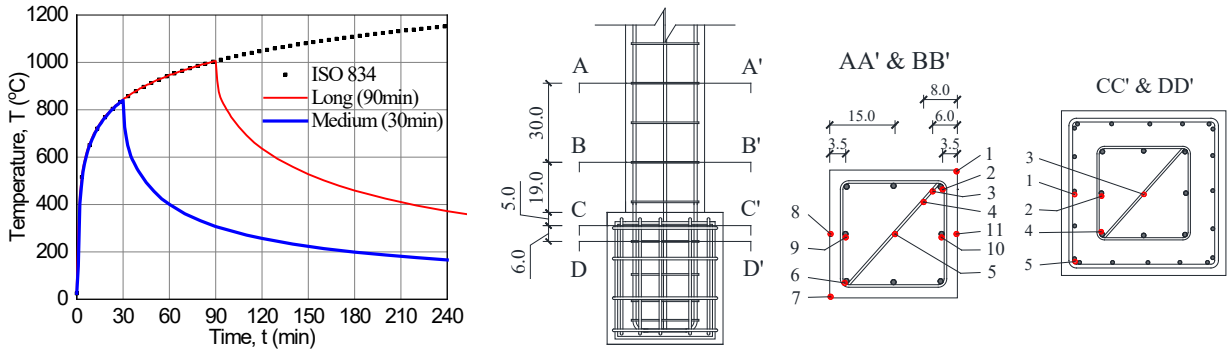

a) b)

Figure 3 – a) ISO 834 and imposed time-temperature curves; b) thermocouples location (dimensions in cm).

2.4. Cyclic loading test setup

The cyclic tests were performed in a purpose-built rig constructed in the Structures Laboratory at Porto University for carrying-out uniaxial and biaxial cyclic tests on reinforced concrete columns with constant or varying axial loads. Figure 4 shows the adopted test set-up arrangement, the idealized support and loading conditions, the adopted monitoring scheme and the lateral displacement path applied at the top column. The test rig includes a vertical 700 kN capacity actuator used to apply the axial compressive load and a horizontal 500 kN capacity actuator with 300 mm stroke to apply the cyclic lateral displacements (d_c). The reaction system for the actuators comprises two stiff steel reaction frames. The column specimen and the reaction frames are fixed to the laboratory strong floor

with pre-stressed steel bars to avoid sliding and overturning of the specimen or sliding of the reaction frame during testing. The axial load actuator remains in a fixed position during the test while the column specimen slides laterally with the help of a sliding device to minimize the friction effects. The sliding device consists of two sliding steel plates, one connected to the axial load actuator (upper plate), which remained fixed, and another connected to the top of the column (lower plate), which was free to displace laterally. A load cell in the horizontal direction is connected to the upper plate to measure the friction force that is subtracted from the force read on the horizontal actuator load cell.

The axial load (N) was set to a constant value of 410 kN which corresponds to an axial load ratio $N/A_g f_{cm}$ = 13.6% for the control column C, where N is the applied axial compressive load, A_g is the gross cross-sectional area of the column and f_{cm} is the concrete compressive strength. The lateral displacements (d_c) are imposed at 1.50 m from the foundation and each demand level cycle is repeated three times, with steadily increasing demand levels. This procedure is adopted to obtain a better understanding of the columns behaviour and allow comparisons between different tests. The adopted lateral load path followed the nominal peak displacement levels of 3, 5, 10, 4, 12, 15, 7, 20, 25, 30, 35, 40, 45, 50, 55, 60, 65, 70, 75, 80 (in mm). The drift values are obtained dividing the lateral displacement by the height of the column (1.50 m). It is noted that the imposed lateral displacements are less than half the cross-section depth. This means that at all drift values the column section remains at least partially under the vertical load actuator, resulting in a constant axial load and negligible P-Delta effects. More information on this test rig can be found at Rodrigues *et al*. [50] and Lucchini *et al.* [51]. The measurement instrumentation includes (1) fourteen potentiometers to measure the local displacements at the column plastic hinge region, (2) four potentiometers to measure the global displacements along the column height, and (3) an inclinometer (located in one lateral face of the foundation) to measure the rotation of the column foundation block. The position of the potentiometers on the two opposite lateral faces of the column (W and E) is presented in Figure 4-c.

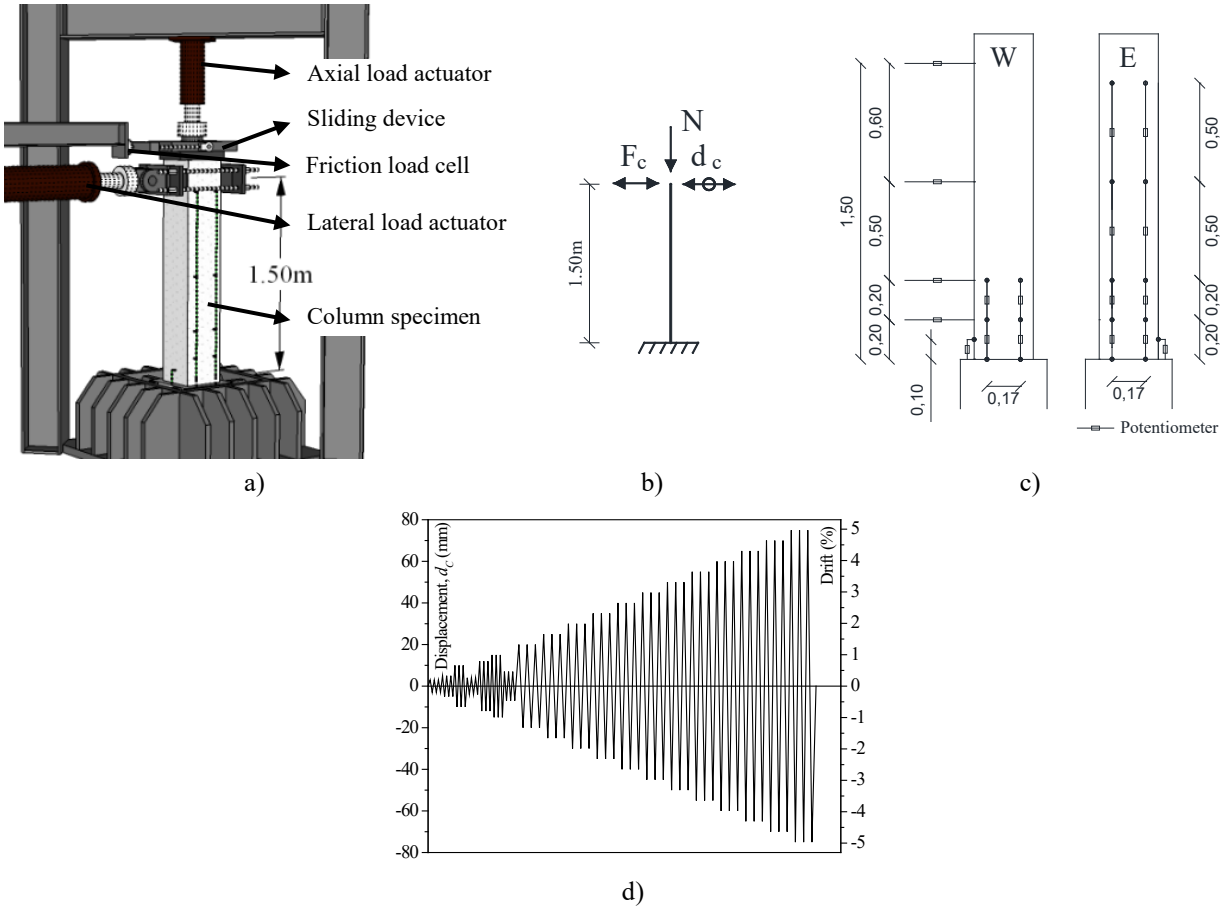

Figure 4 – a) test setup; b) loading conditions idealized; c) monitoring scheme (dimensions in meters); d) lateral displacement path.

3. Fire exposure results

3.1. Temperature evolution

The temperature evolution within the columns during the medium and long fire exposure and cooling stages are shown in Figure 5 and Figure 6, respectively. These show the envelope of all thermocouple measurements at each location for both cross-sections AA' and BB', and for both specimens exposed to the same fire duration (i.e. a set of eight readings for each of locations 1&7, 2&6, 8&11, and 9&10; and a set of four readings for locations 3, 4, and 5). The gas phase temperature measured by the controlling plate thermometers is also plotted in Figures 5 and 6. The mean plate thermometer temperature coincides with the prescribed ISO 834 time-temperature curve, whereas error bars indicate the envelope of the four plate thermometer measurements (a standard deviation up to ±38ºC). However, it should be noted here that the plate thermometers were logged by & controlled the furnace

at one minute intervals, and the actual gas phase temperature during the first minutes of exposure may have been somewhat more severe compared to the prescribed curve. This may have also been exaggerated by the fact that plate thermometer measurements may display some lag during this highly transient stage of the fire due to the thermal inertia of their back-insulated steel plate [52], thus underestimating the actual gas phase temperature experienced by the columns in the beginning of fire exposure. This is evidenced by the temperature spikes measured by the embedded thermocouples at the corners and surface of the columns (logged at a frequency of 1 Hz) as shown in Figures 5(a) and 6(a).

At the corners (locations 1&7) and the centre of the exposed column face (locations 8&11), temperatures followed in general those of the gas phase closely. The peak average temperature at the end of the 30 min heating phase was 772ºC (standard deviation ±41ºC) at the corner and 734ºC ±39ºC at surface centre of columns M and M-S. The respective temperatures for columns L and L-S at the end of the 90 min heating phase were 967ºC ±16ºC and 949ºC ± 15ºC. In the concrete, temperatures increased at a slower rate and continued to increase even after the decay phase of the fire exposure had started. The temperature development within the core was also delayed due to the distinct plateau that is observed near 100ºC, due to the migration and evaporation of moisture. Following the 30 min fire exposure, the centre of the concrete core reached a peak temperature of 153ºC ±12ºC after approximately 4 hours (280 minutes from start of the heating). In the case of the 90 min exposure, peak temperatures in the core reached 348ºC ±27ºC at 320 minutes from the start of the heating. Rebar temperatures reached in the case of the medium fire 261ºC ±22ºC at the corners and 196ºC ±14ºC at the middle rebar; in the case of the long fire these were 496ºC ±13ºC and 416ºC ±24ºC, respectively, hence it can be assumed that the degradation in their mechanical properties during fire has fully recovered upon cooling down to ambient, since they did not substantially exceed 500ºC [2]. It is noteworthy that although corner rebars have somewhat larger concrete cover than middle bars (due to the bending radius of the stirrup), they still heat up faster and reach higher temperatures due to the two-dimensional heat transfer at the corners, in contrast to the one-dimensional heat transfer

across the section's centreline. At the end of the cooling phase when the furnace was opened 24 hours later, temperature was almost the same in all thermocouples (approximately 100ºC).

From the temperature evolutions shown in Figures 5 and 6, it is evident that relatively large discrepancies were measured between individual thermocouples at each location. Standard deviations as high as 175ºC were recorded for the outermost thermocouples at the beginning of the heating phase; for thermocouples at or near the rebar, standard deviations were up to 50ºC. No correlation was observed between thermocouple locations at the two different cross-sections (i.e. with respect to height from the column base), thus it can be assumed that heat transfer in these regions is two-dimensional and the influence of the insulated foundation block is insignificant. The primary reason for the large discrepancy between thermocouples is most likely the positioning accuracy of their tips within zones characterised by high thermal gradients. These could have been exaggerated by (even slight) displacements of the thermocouple tips during concrete casting. Furthermore, the plate thermometer temperature variation indicates a potential spatial variation of temperature within the furnace (as opposed to the common assumption of uniform furnace temperature due to the highly turbulent flow of hot gases around the specimen). This could have caused slightly non-uniform incident heat fluxes on the columns' surfaces, thus also affecting – to some extent – the propagation (and symmetry) of the 'thermal wave' within the cross-section and the temperature development measured by the thermocouples. However, the latter is only a speculation that requires further investigation and cannot be verified from the current test measurements.

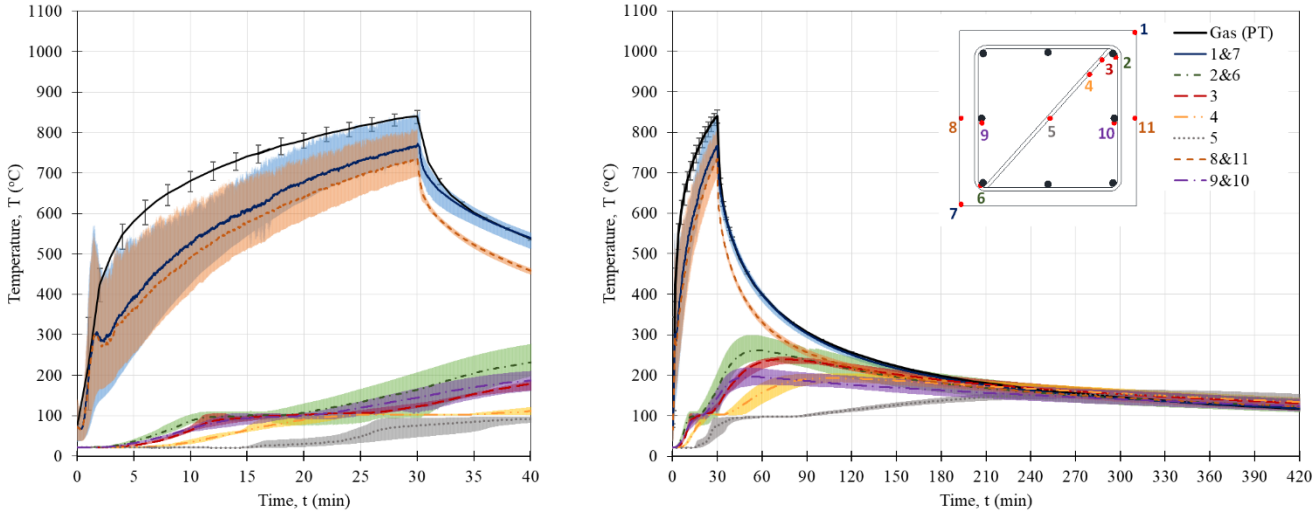

Figure 5 – Temperature evolution during the 30 min fire exposure for specimens M and M-S. Envelopes and trend lines of the mean temperature are shown at the respective location for all thermocouples in cross-sections AA' and BB'; (a) and (b) show the same data at different timescales.

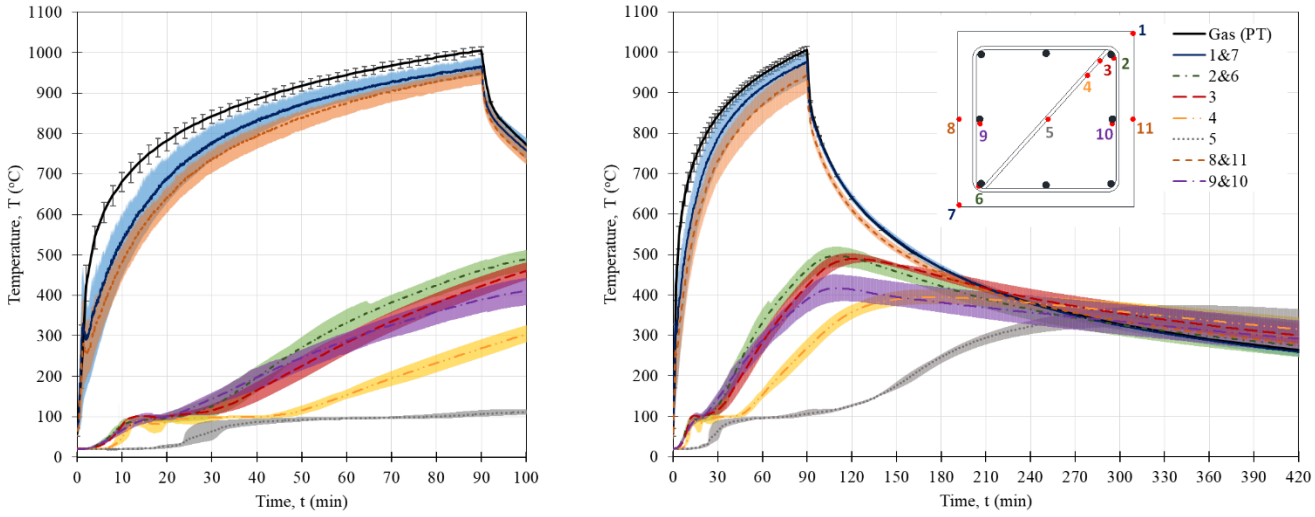

Figure 6 – Temperature evolution during the 90 min fire exposure for specimens L and L-S. Envelopes and trend lines of the mean temperature are shown at the respective location for all thermocouples in cross-sections AA' and BB'; (a) and (b) show the same data at different timescales.

No significant heat penetration was observed within the insulated foundation block. For columns M and M-S, the measured peak temperatures ranged between 73-79°C in section CC' and 61-72°C in section DD'. For columns tested under the long fire, the maximum temperature observed in section CC' ranged between 134°C-165°C, whereas a similar variation was observed in section DD', but with lower temperatures by approximately 20°C.

The maximum temperature measured by the thermocouples placed in the cross-section diagonal (from point 1 to point 7) are shown in Figure 7. It is noted that Figure 7 presents the peak temperatures

experienced at each location throughout the whole fire exposure and cooling duration (i.e. they do not correspond to the same time point at each location, due to the propagating thermal wave). Linear branches were used between the discrete data points to represent the trend of the actual peak temperature profile.

To quantify the actual peak temperature distribution across the whole cross-section of the exposed columns, a heat transfer analysis was performed using the finite element analysis software Abaqus FEA and validated against the thermocouple measurements at locations 1 to 11. Figure 7 shows that the predicted peak temperatures from the heat transfer analysis are in good agreement with the experimental measurements. The distribution of the maximum temperatures experienced in the exposed sections during the medium and long fire are shown in Figure 8. Assuming the simplistic compressive strength reduction factors provided by Eurocode 2 [5] for concrete with calcareous aggregates at elevated temperature, and the additional reduction factors upon cooling provided by Eurocode 4 [53], these temperature distributions result in an estimated reduction in the axial load bearing capacity of the column by 16.7% and 35.4% for the medium and long fire exposure, respectively.

The heat transfer analysis considered a 2D quarter-symmetry model of the column cross-section discretised by 4-node linear heat transfer quadrilateral (DC2D4) elements with a size of 2 mm. Radiation and convection at the exposed surface were modelled in Abaqus as surface radiation and surface film condition interactions, respectively. The emissivity of concrete was taken as 0.7 and the convection factor as 25 W/m^2K, whereas the ambient temperature was specified as the respective gas phase temperature measured by the PTs in the medium and long fire tests. The thermal properties adopted for concrete and steel were those recommended in Eurocode 2 [5], assuming lower limit values for the thermal conductivity of concrete and a moisture content of 5% for the peak value accounting for water evaporation in the respective function of the specific heat.

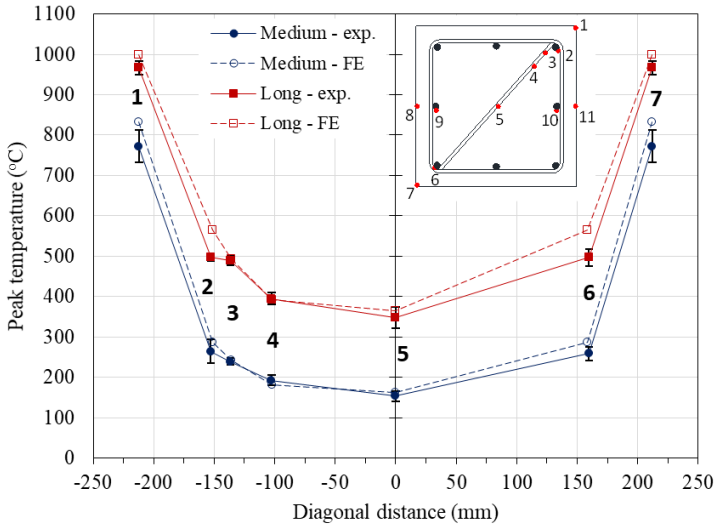

Figure 7 – Maximum temperature profile at diagonal cross-section.

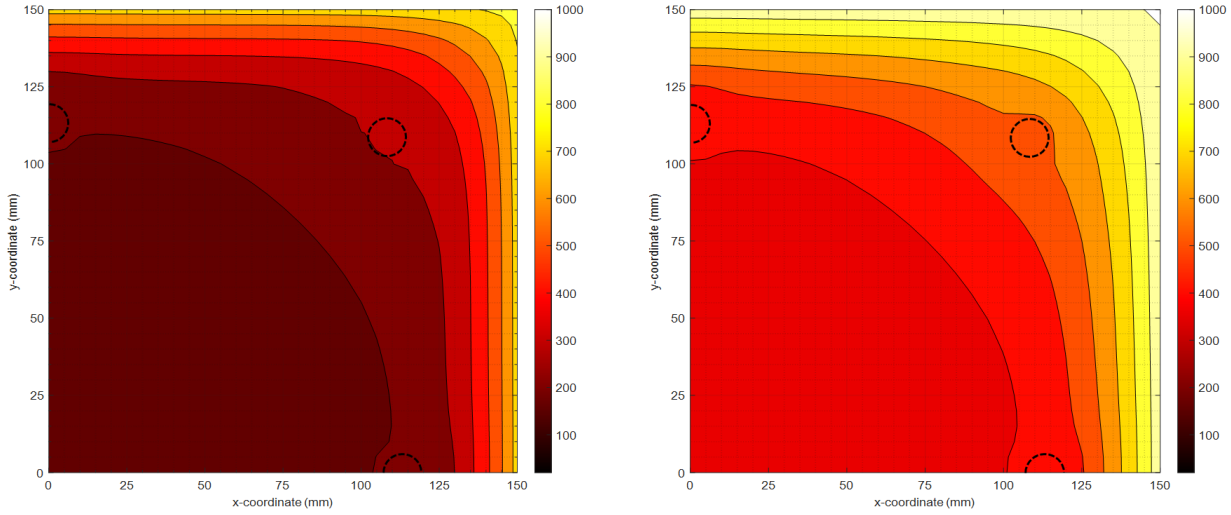

(a) (b)

Figure 8 – Predicted distribution of the maximum temperatures reached within sections AA' and BB' during the (a) medium and (b) long fire exposures. (Quarter of the cross-section shown, with rebar locations annotated).

3.2. Damage observations after fire exposure

Figure 9 shows the condition of the columns after opening the furnaces upon cooling down. After the medium fire the columns appeared only lightly damaged, with fine transverse and longitudinal cracks near the corners and moderate crazing of the cement paste all over the exposed column surface. Some slight discolouration of the concrete surface was apparent in comparison with the insulated parts of the specimen, except for a zone of approximately 25-30mm around the corners, where the colour was distinguishably whitish-grey and the cement paste had disintegrated. This is due to the disintegration

of the calcareous constituents of cement and the limestone aggregates at temperatures greater than 800ºC [3], whereas the extent of this zone is in agreement with the temperature distribution shown in Figure 8(a). It is interesting to note that in practice, based only on visual inspection the columns subjected to medium fires do not appear badly damaged. An inexperienced building owner might not therefore see the need to strengthen the column post-fire.

The columns that were exposed to the long fire were first examined immediately upon opening the furnace 24 hours after the fire exposure. In this case, the column corners were extensively cracked over a wider (>100mm) distinctly whitish-grey decarbonated zone, whereas the remaining of the column surface was extensively crazed and discolourised. In a further inspection of the columns three days later, a layer of approximately 10-20 mm of concrete had flaked and popped off (Figure 9-b), due to the expansive rehydration of the dissociated limestone aggregates and calcium carbonate constituents (i.e. calcium oxide, after exposure to beyond 800ºC) [1, 2] from interaction with the ambient air. Furthermore, large longitudinal cracks opened at the corners up to the rebar level, resulting in vertical wedge-like pieces separating (and in some cases falling off completely) from the column. This cracking pattern is due to differential thermal expansion between the inner and outer zones of concrete and was also observed in previous studies; Lie et al. [27] attributed this to the ongoing expansion of inner core which is still heating up while the outer zones are cooling down during the decay phase of the fire. However, concrete fracture in this zone is also likely to occur during the heating stage because of the restrained expansion of the hot outer layers by the cooler inner core, with further mobilization of the fracture planes happening during cooling due to the reversal of thermal gradient, as well as the physicochemical changes upon cooling due to rehydration of the disintegrated concrete constituents described above. However, the exact mechanisms of cracking are beyond the scope of the current paper and are a subject of future numerical investigations.

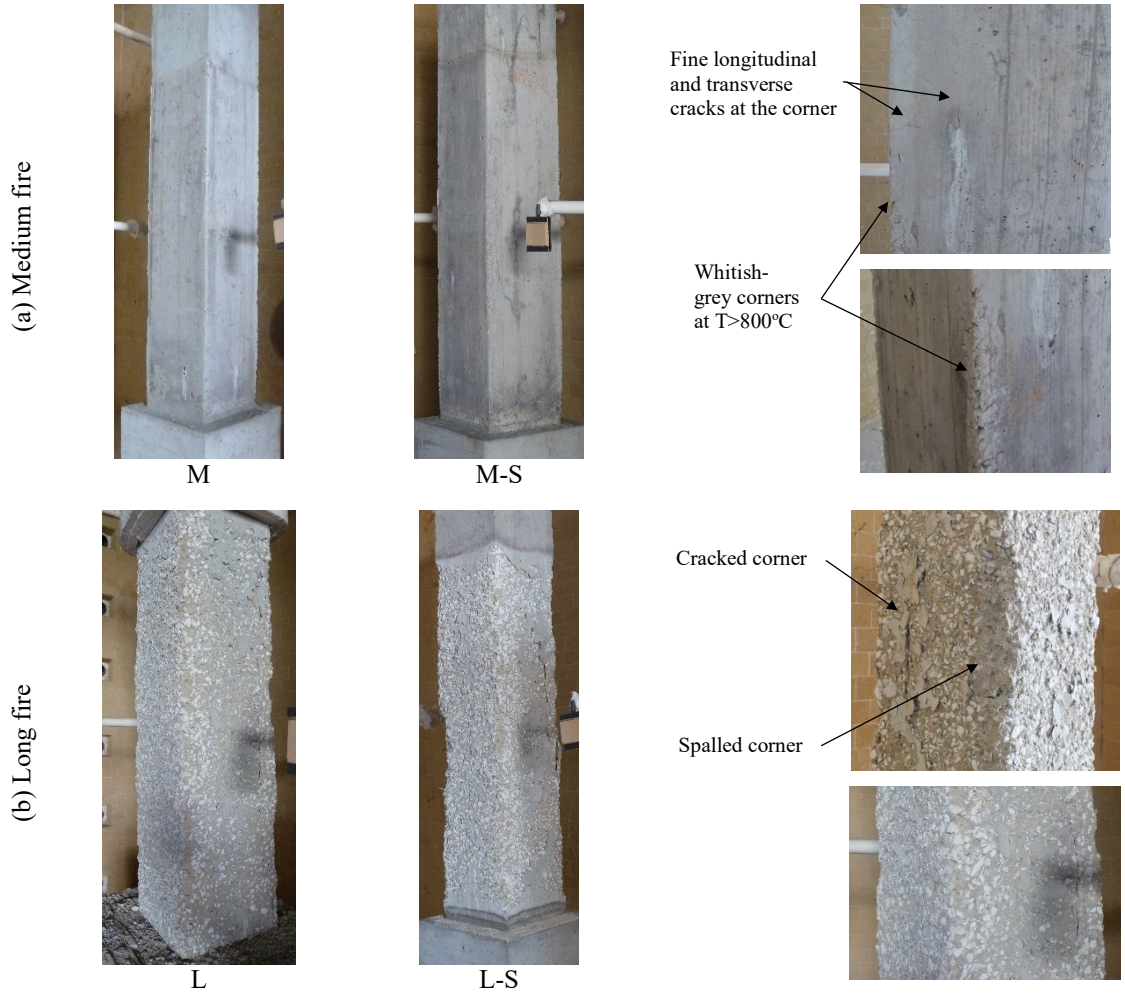

Figure 9 – Visual appearance of specimens after fire testing.

4. Repairing and strengthening of the columns

Columns M-S and L-S were repaired by replacing the hollow-sounding and weak concrete layers which had been exposed to temperatures greater than approximately 550-600ºC, with a new structural repair mortar as demonstrated in Figure 10. In column M-S only the cracked and overheated corners of the concrete cover were removed, while in column L-S the whole concrete cover was removed to the depth of the longitudinal reinforcement. The damaged concrete was replaced by a R4 class structural mortar according to EN1504-3 [54] with a minimum compressive strength of 45 MPa. The original cross-section dimensions of the columns were reinstated, and the edges were rounded to a radius of 25 mm to increase the confinement efficiency of the CFRP wrap. After 3 weeks of curing, no shrinkage cracks were observed in the columns. In the strengthened control column C-S, the edges were also rounded to a radius of 25 mm before wrapping with CFRP. In all strengthened columns,

the concrete surface was roughened and cleaned, and then a wet-layup CFRP fabric (300 mm width) impregnated and bonded with epoxy resin was used for wrapping the columns.

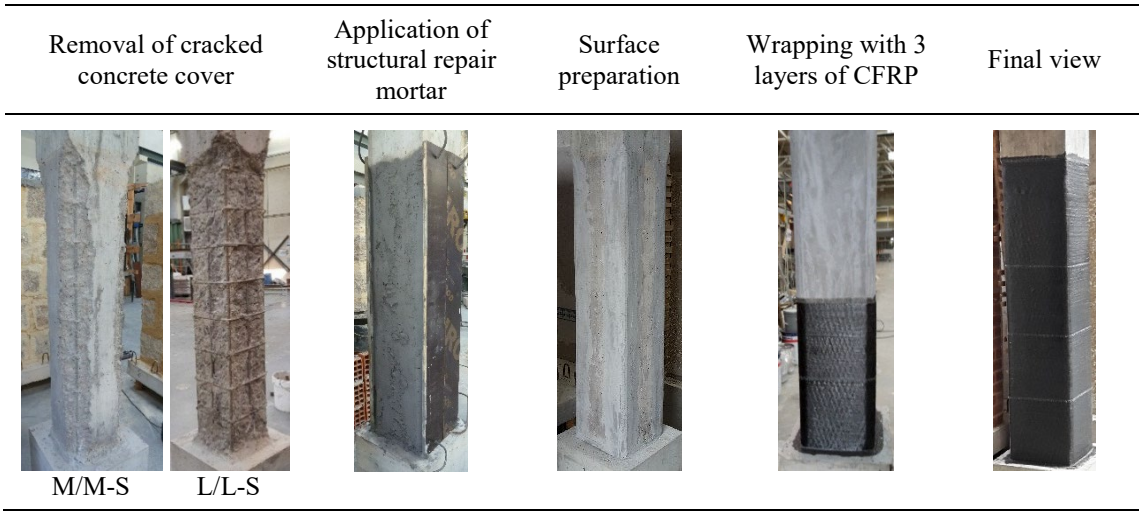

Figure 10 – Repair and strengthening process.

The repair and strengthening design of the columns aimed to reinstate the original flexural capacity of the columns and increase their ductility, respectively, and in so doing, improve their energy dissipation capacity and consequently their seismic performance. To this end, the columns were wrapped with three layers of a unidirectional CFRP sheet to their full height to increase the concrete confinement (see Figure 10). The strengthening scheme was designed and detailed according to the Italian CNR-DT-200.R1/2013 [55] guideline. The wrapping method followed the same procedure already implemented in columns of beam-column joint specimens [56]. The CFRP sheet properties were: design thickness (t_f) – 0.168 mm; ultimate strength ($f_{u,FRP}$) – 4300 MPa; ultimate strain ($\varepsilon_{u,FRP}$) – 1.7%; and elastic modulus (E_{FRP}) – 240GPa. Considering only the confinement effect given by the three layers of CFRP, the confined concrete compressive strength was 43.8 MPa (+31% than the unconfined concrete) for column C-S.

It should be noted that the fire performance of the FRP-strengthened column is not treated explicitly herein. Although this paper is concerned with the effects of earthquake as a subsequent hazard acting on a fire-damaged and repaired structure, fire remains a credible hazard for the columns' extended service life after strengthening. Therefore, a verification of the strengthened column's structural resistance for the fire limit state according to relevant structural design codes [5] and guidance [57, 58] is also necessary. For the strengthening levels of the particular columns examined in this study

(i.e. reinstatement of their original capacity after damage), the underlying reinforced concrete cross-section maintains sufficient capacity to resist gravity loads during the considered standard fire durations, even if the FRP wrap is neglected (i.e. it becomes ineffective in fire). In fact, the latter is a reality that applies in many practical design cases of FRP-strengthened concrete members since the actions considered in the (accidental) fire limit state are considered in design as being reduced when compared to those of the ultimate limit state at ambient temperature; for most buildings, load ratios (member utilisation ratios) are typically less than 0.5 [59]. It is noteworthy that, in case the unstrengthened column's capacity is insufficient to meet the fire resistance requirements for increased imposed loads after strengthening, supplemental insulation [60, 61] or novel hybrid strengthening/fire-protecting composite systems [62] can be installed to improve fire performance following the design philosophy for structural fire resistance outlined in [57, 58].

5. Cyclic test results

5.1. Lateral force vs drift

The effect of previous fire on the cyclic performance of the columns is evaluated by direct comparison between the results obtained in the cyclic tests of the fire damaged columns (M and L) with the control column (C) as shown in Figure 11-a,b. In the case of the 30-minute fire exposure, the cyclic behaviour of column M shows a reduction in initial stiffness but a similar peak force and ductility as the control specimen. In the case of the 90-minute fire, a reduction in initial stiffness as well as a significant reduction in peak force and column ductility are observed in column L as compared to the control specimen. The repaired and strengthened columns, M-S and L-S, show similar lateral peak force, lower initial stiffness and a significantly larger deformation capacity as compared to the control column C (see Figure 11-b,c). This demonstrates that the repair and CFRP wrapping were efficient in minimising the effects of previous fire damages and in improving the cyclic deformation and energy dissipation capacity of the columns.

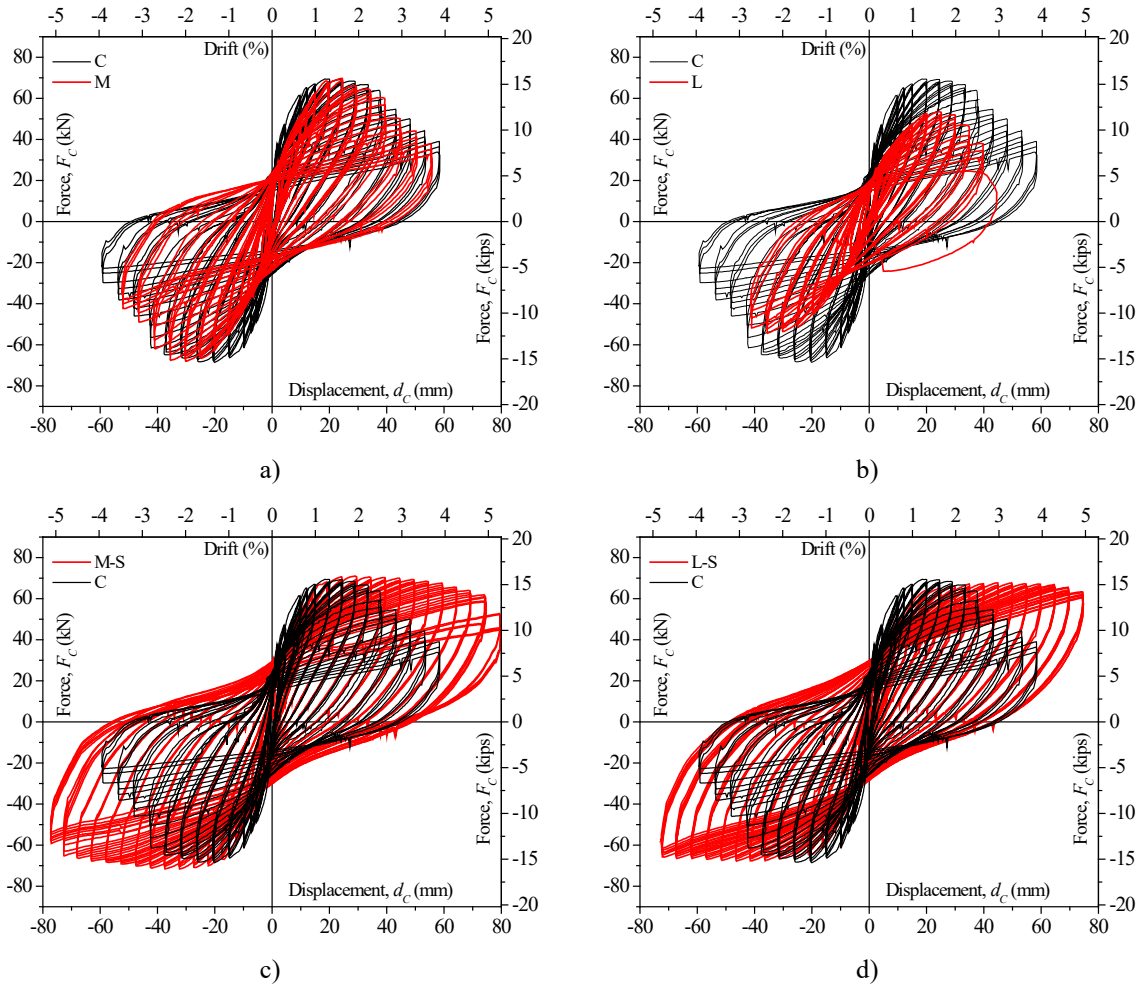

Figure 11 – Lateral load-displacement relationship: a) C and M; b) C and L; c) C and M-S; d) C and L-S.

The strengthened columns with fire damage (M-S and L-S) reached lower peak loads and had lower initial stiffnesses than the strengthened control column (C-S) (see Figure 12). The unloading-reloading stiffness, and consequently the pinching effect, is similar for all the strengthened columns.

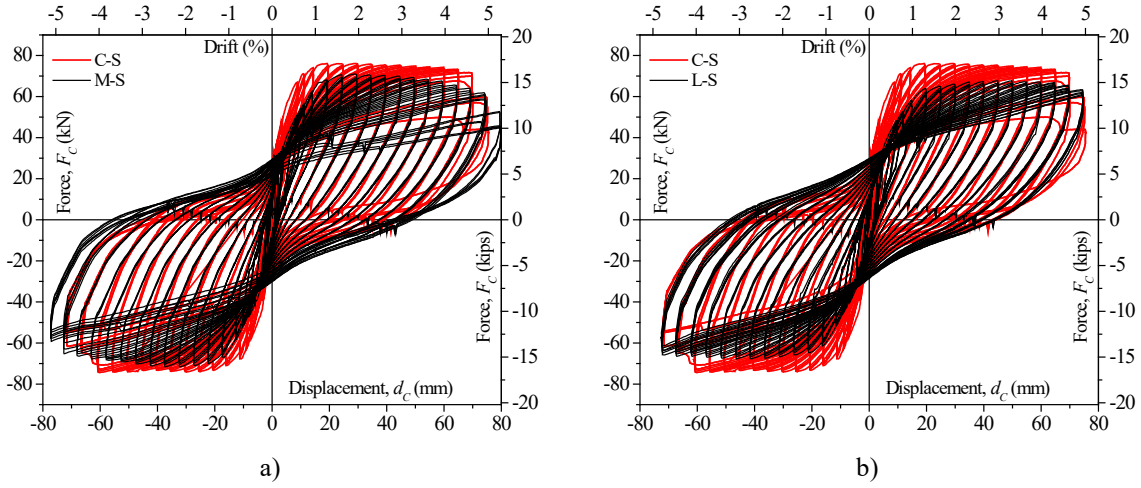

Figure 12 – Lateral load-displacement relationship: a) C-S and M-S; b) C-S and L-S.

The envelopes of the cyclic lateral load-displacement relationships are plotted in Figure 13 and more clearly show the larger initial stiffness of the control columns when compared to the fire damaged columns. The figure also shows that all repaired and strengthened columns had higher deformation capacity and a more ductile behaviour than the non-strengthened columns.

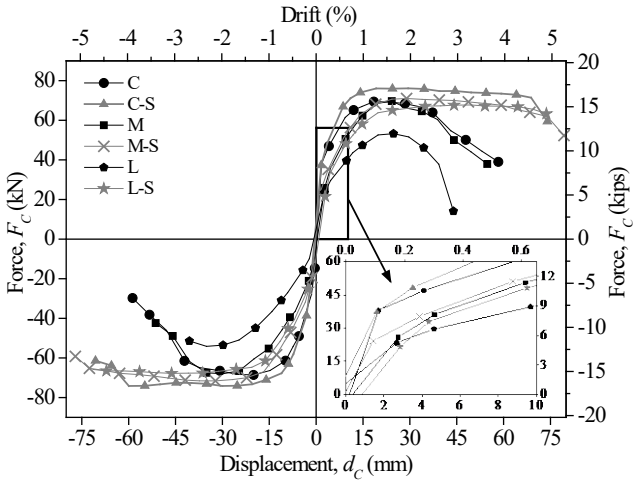

Figure 13 – Lateral load-displacement envelopes.

Table 3 presents the results of the cyclic test main values (for positive direction), including the peak lateral force $F_{c,max}$, the drift at peak force $d_{c,max}$, the ultimate force $F_{c,ult}$, the drift at ultimate force $d_{c,ult}$, the drift at yield $drift_y$, and the displacement ductility at ultimate point $\mu_{\Delta,ult}$. The ultimate point is conventionally taken as the point at which a strength drop of 20%, relative to the maximum force $F_{c,max}$, is observed as adopted by Park and Ang [63]. The yield displacement was determined assuming the elastic-perfectly plastic force–displacement relationship according to Annex B.3 of EC8-1 [64]. For each column, an elastic-perfectly plastic relationship was fitted to the experimental lateral load – displacement envelope up to the ultimate point, ensuring the following requirements were satisfied: (i) the areas under and above the experimental envelope curve must have the same values; and (ii) the area under (or above) the envelope curve is the lowest possible [65]. The displacement ductility at ultimate point is the ratio between the ultimate drift and drift at yield. The strength reduction after peak observed in column L-S was only 6.5% and was limited by the capacity of the test rig, hence, for this column the conventional ultimate point was not reached.

Table 3 – Force and drift values at peak, drift at ultimate point, drift at yield and ductility at ultimate point.

Column	$F_{c,max}$ (kN)	$d_{c,max}$ (%)	$F_{c,ult}$ (kN)	$d_{c,ult}$ (%)	$drift_y$ (%)	$\mu_{\Delta,ult}$
C	69.4	1.2	55.5	2.8	0.38	7.4
C-S	76.1	1.3	60.9	4.9	0.37	13.2
M	69.7	1.6	55.8	2.7	0.65	4.2
M-S	71.0	1.9	56.8	5.1	0.64	7.9
L	53.2	1.7	42.6	2.4	0.96	2.5
L-S	67.7	3.3	-	-	0.82	-

Similar values of $F_{c,max}$ were observed in columns C and M. Instead, columns L, C-S, M-S and L-S achieved -23%, +10%, +2% and -2% of the $F_{c,max}$ *of* column C, respectively. The $F_{c,max}$ of columns M-S and L-S were -7% and -11% of that of column C-S. Therefore, the effect of previous fire damage, in terms of peak force, were only evident in column L and the adopted strengthening technique was able to re-instate the original peak strength. The differences in displacement ductility between column C and columns M, L, C-S and M-S were -44%, -66%, +79% and +8%, respectively. The fire damage significantly reduced the displacement ductility capacity of the columns, namely from 7.4 (column C) to 4.2 for column M and 2.5 for column L. The ultimate drift and displacement ductility at ultimate point observed in the strengthened columns were considerably larger (almost double) than those of the control column C. This demonstrates the efficiency of the CFRP wrapping for increasing the deformation capacity of the columns and decreasing the softening effect.

The strength degradation-drift between the first and second cycles of each drift level, and between the first and third cycles of each drift level are shown in Figure 14. The strength degradation follows two different trends: (1) the columns without CFRP wrapping show an increasing strength degradation for large drift demands, while (2) in the strengthened columns the strength degradation is almost a constant value (average of 1.8% for $SD_{1\text{-}2}$ and 3.3% for $SD_{1\text{-}3}$) up until 4% drift, and then increases significantly.

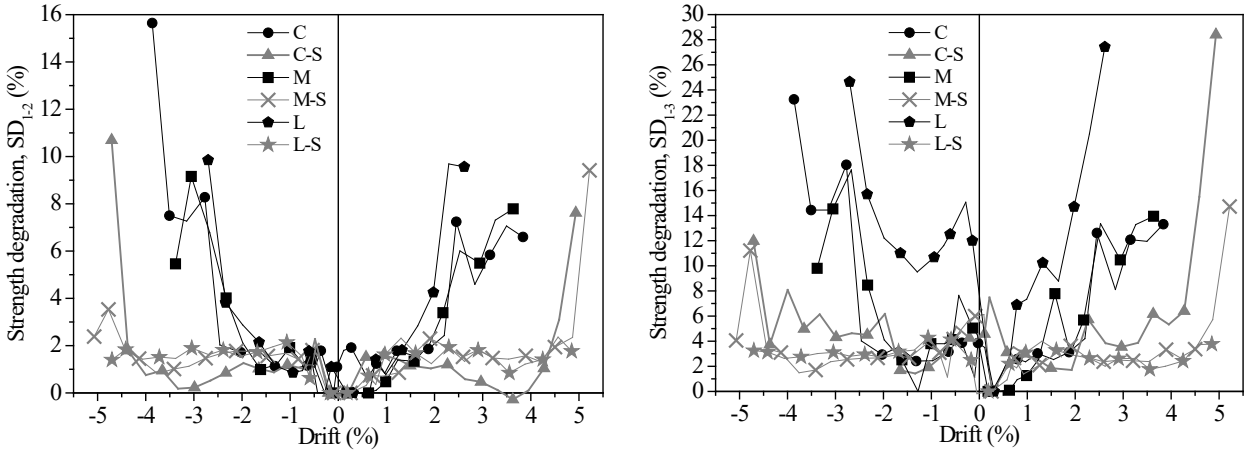

Figure 14 – Strength degradation: a) between cycles 1 and 2; b) between cycles 1 and 3.

As observed in Figure 13, fire exposure influences the stiffness of the column, especially in column L, due to the degradation of concrete modulus and strength in the outermost regions of the cross-section. The secant stiffness-drift relationship is presented in Figure 15, where secant stiffness (K) is calculated dividing $F_{c,max}$ by $d_{c,max}$ (converted to displacement) for the first positive displacement at each displacement level (Figure 4). As expected, columns C, and C-S present the largest initial stiffnesses, as they sustained no fire damage. However, column L-S where the damaged concrete cover was totally replaced by structural repair mortar, also shows a comparably large stiffness. The initial stiffness of columns M and L are only 75% and 40% of the one observed in the control column C. After 1% drift the secant stiffness evolution is almost coincident in the strengthened columns and is significantly lower in column L.

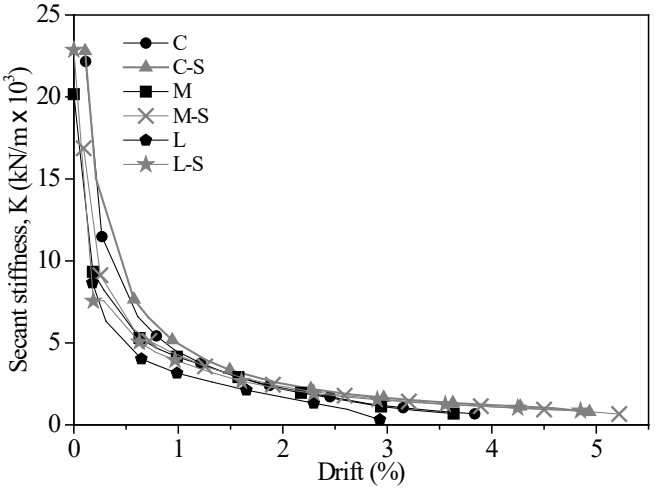

Figure 15 – Secant stiffness evolution.

5.2. Dissipated energy evolution

The evolutions of the total hysteretic dissipated energy with increasing drift for the columns are shown in Figure 16. The dissipated energy evolution is computed as the sum of the energy dissipation associated to each hysteretic cycle and corresponds to the interior area of the force-displacement loops. The cumulative hysteretic dissipated energy values at the ultimate drift are distinctly marked in Figure 16 and for columns C, M, L, C-S and C-M, were respectively 53.7 kNm, 45.1 kNm, 25.0 kNm, 175.5 kNm and 187.7 kNm. Columns M and L dissipated 16% and 53% less energy than the control column C up to the ultimate drift and columns C-S and M-S dissipated 227% and 250% more energy than column C. Therefore, the fire induced damage decreases the energy capacity of the columns. On the other hand, the CFRP wrapping increases significantly the dissipated energy capacity for cyclic lateral loading.

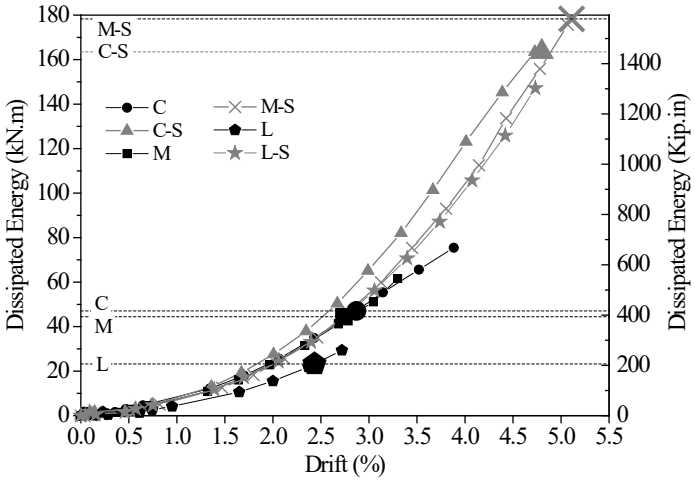

Figure 16 – Dissipated energy evolution.

5.3. Observed damage

The observed damage at the end of each column cyclic test is illustrated in Figure 17. Only damage associated to bending in the plastic hinge region is observed, namely: flexural concrete cracks, concrete cover spalling, buckling of the longitudinal reinforcing bars and concrete failure in compression. Buckling occurred due to the poor confinement associated to the large stirrup spacing. In column C the cracks were spread along the column to a height of 60cm from the foundation, with concrete cover spalling and the buckling of reinforcing bars occurring at the base of the column. In column M the concrete cracks extended over a shorter length (50 cm from column base) and the

concrete spalling was greater than in column C. In column L it was not possible to identify the concrete cracks due to the irregularities and fire damage on the concrete faces, however concrete spalling was observed, the longitudinal reinforcing bars buckled and the concrete was observed to fail in compression due to cross section concrete loss (concrete cover and core crushing during the cyclic loading) and axial load. In the strengthened columns it was not possible to observe the damage due to the CFRP wrapping, apart from the visible bulging of the wrap due to the large compressive strains (and possibly, the restrained buckling of the middle rebar) at high rotations.

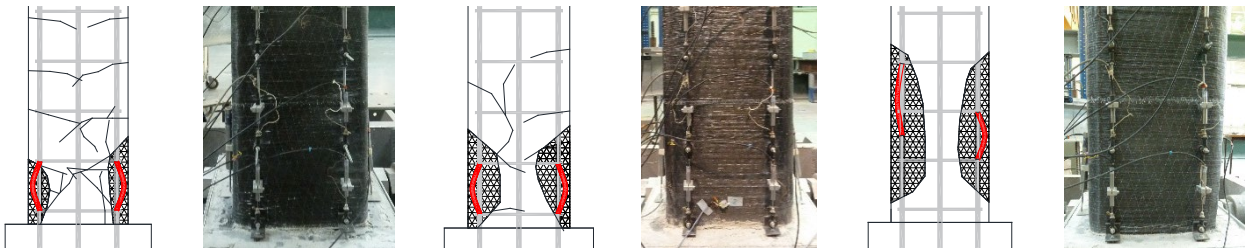

Figure 17 – Damage observed at the end of each test.

6. Conclusions

An experimental campaign on six full-scale reinforced concrete specimens, representative of existing columns, was carried out to assess the seismic behaviour of these elements post-fire and after strengthening post-fire. The fire tests were performed in a furnace following the ISO 834 fire curve up to 30 or 90 minutes and then allowed to cool. Half of the specimens were repaired and strengthened with CFRP wrapping to improve the concrete confinement and consequently increase the column ductility capacity for uniaxial lateral cyclic loading. Based on the experimental results, the following conclusions can be drawn:

- The medium fire exposure (30 minutes) resulted in moderate damage to the columns limited to the corners of the concrete cover. On the other hand, after the long fire exposure (90 minutes) extensive cracking and disintegration of the whole concrete cover was observed.
- The post-fire cyclic behaviour of column M showed a lower initial stiffness when compared with the control specimen C but sustained a comparable peak force. However, in column L

significantly lower initial stiffness, peak force and ultimate displacement were observed. Consequently, the displacement ductility of columns M and L was respectively 44% and 66%, lower than the control column C, whereas the respective reduction in dissipated energy was 16% and 53%. This shows that the cyclic response of column L was severely compromised by the long fire, which justifies the need for the column to be strengthened after the fire.

- Columns M-S and L-S, which were repaired and strengthened with CFRP wrapping after fire, showed better cyclic performance than the control column C, once the cumulative energy dissipation was 227% and 250% greater than column C, respectively.
- The repair and strengthening method studied herein is demonstrated to improve the cyclic behaviour of the columns after a medium (30 mins of ISO-834) or long fire (90 mins of ISO-834) and it can result in a significantly improved seismic response even compared to the undamaged original column. It is also shown that the post-fire strengthened columns can achieve a similar seismic performance than an analogous strengthened column without previous fire damage.

This paper contributes to the state-of-art by adding to the few experimental data currently available on the post-fire seismic behaviour of RC elements. Moreover, it presents innovative experimental data of post-fire strengthened RC columns tested under lateral cyclic loading. Future work will use these experiments to validate numerical models of RC structures subjected to sequential fire and earthquake loads.

7. Acknowledgments

This research was conducted as part of the Challenging RISK project funded by the UK Engineering and Physical Science Research Council - EPSRC (EP/K022377/1) for which Prof. Tiziana Rossetto and Prof. Luke Bisby are Principal Investigators at UCL and University of Edinburgh, respectively. The work developed by the author José Melo was partly financially supported by FCT - Fundação para a Ciência e Tecnologia, Portugal, co-funded by the European Social Fund, namely through the post-doc fellowship, with reference SFRH/BPD/115352/2016 and by Base Funding -

UIDB/04708/2020 and Programmatic Funding - UIDP/04708/2020 of the CONSTRUCT - Instituto de I&D em Estruturas e Construções - funded by national funds through the FCT/MCTES (PIDDAC).

8. References

1. Bailey, B.G. and G.A. Khoury, *Performance of Concrete Structures in Fire*. 2011: Camberley, United Kingdom.
2. International Federation for Structural Concrete (*fib*), *fib Bulletin 46: Fire design of concrete structures - structural behaviour and assessment*. 2008, International Federation for Structural Concrete (*fib*): Lausanne, Switzerland. p. 209.
3. The Concrete Society, *Technical Report No. 68: Assessment, Design and Repair of Fire-damaged Concrete Structures*. 2008: Camberley, United Kingdom.
4. BSI, *BS EN 1991-1-2:2002. Eurocode 1: Actions on structures — Part 1-2: General actions - Actions on structures exposed to fire*. 2002, British Standards International: London, United Kingdom.
5. BSI, *BS EN 1992-1-2:2004. Eurocode 2: Design of concrete structures — Part 1-2: General rules — Structural fire design*. 2004, British Standards International: London, United Kingdom.
6. Bisby, L.A., H. Mostafaei, and P. Pimienta, *White Paper on Fire Resistance of Concrete Structures*. 2014, Gaithersburg, MD: National Institute of Standards and Technology (NIST).
7. Bisby, L., J. Gales, and C. Maluk, *A contemporary review of large-scale non-standard structural fire testing.* Fire Science Reviews, 2013. **2**(1): p. 1-27.
8. Ioannou, I., et al., *Expert judgment-based fragility assessment of reinforced concrete buildings exposed to fire.* Reliab. Eng. Syst. Saf., 2017. **167**: p. 105-127.
9. Rush, D. and D. Lange, *Towards a fragility assessment of a concrete column exposed to a real fire – Tisova Fire Test.* Engineering Structures, 2017. **150**: p. 537-549.
10. Ioannou, I., et al., *Expert judgment-based fragility assessment of reinforced concrete buildings exposed to fire.* Reliability Engineering & System Safety, 2017. **167**: p. 105-127.
11. Molkens, T., R. Van Coile, and T. Gernay, *Assessment of damage and residual load bearing capacity of a concrete slab after fire: Applied reliability-based methodology.* Engineering Structures, 2017. **150**: p. 969-985.
12. BSI, *BS EN 1998-1:2004. Eurocode 8: Design of structures for earthquake resistance – Part 1: General rules, seismic actions and rules for buildings*. 2004, British Standards International: London, United Kingdom.
13. BSI, *BS EN 1998-3:2005. Eurocode 8: Design of structures for earthquake resistance – Part 3: Assessment and retrofitting of buildings* 2005, British Standards International: London, United Kingdom.
14. Fardis, M.N., *Seismic Design, Assessment and Retrofitting of Concrete Buildings*. Geotechnical, Geological, and Earthquake Engineering. 2009, Dordrecht: Springer. 744.
15. Kamath, P., et al., *Full-scale fire test on an earthquake-damaged reinforced concrete frame.* Fire Safety Journal, 2015. **73**: p. 1-19.
16. Shah, A.H., et al., *Fire performance of earthquake-damaged reinforced-concrete structures.* Materials and Structures, 2016. **49**(7): p. 2971-2989.
17. Behnam, B. and H. Ronagh, *A Post-Earthquake Fire Factor to Improve the Fire Resistance of Damaged Ordinary Reinforced Concrete Structures.* Journal of Structural Fire Engineering, 2013. **4**(4): p. 207-226.
18. Vitorino, H., H. Rodrigues, and C. Couto, *Evaluation of post-earthquake fire capacity of reinforced concrete elements.* Soil Dynamics and Earthquake Engineering, 2020. **128**: p. 105900.
19. Jian-Zhuang Xiao, J.L. and H. Zhan-Fei, *Fire Response of High-Performance Concrete Frames and Their Post-Fire Seismic Performance.* ACI Structural Journal, 2008. **105**(5).
20. Xiao, J., et al., *Fire Resistance and Post-fire Seismic Behavior of High Strength Concrete Shear Walls.* Fire Technology, 2017. **53**(1): p. 65-86.
21. Li, L.-Z., et al., *Experimental study on seismic performance of post-fire reinforced concrete frames.* Engineering Structures, 2019. **179**: p. 161-173.

22. Demir, U., et al., *Effect of Fire Damage on Seismic Behavior of Cast-in-Place Reinforced Concrete Columns.* Journal of Structural Engineering, 2020. **146**(11): p. 04020232.
23. Wang, Y., et al., *Seismic Performance of Reinforced Concrete Frame Joints after Exposure to Fire.* ACI Structural Journal, 2021. **118**(3).
24. Mo, Y.L., C. Hwang, and J. Wang, *Seismic Response of Fire-Damaged Reinforced Concrete Buildings.* Advances in Structural Engineering, 2004. **7**(1): p. 95-109.
25. Mostafaei, H., F.J. Vecchio, and N. Bénichou, *Seismic Resistance of Fire-Damaged Reinforced Concrete Columns*, in *Improving the Seismic Performance of Existing Buildings and Other Structures*. 2009. p. 1396-1407.
26. Ni, S. and A.C. Birely, *Post-fire seismic behavior of reinforced concrete structural walls.* Engineering Structures, 2018. **168**: p. 163-178.
27. T. T. Lie, T. J. Rowe, and T.D. Lin, *Residual Strength of Fire-Exposed Reinforced Concrete Columns.* ACI Symposium Publication. **92**.
28. Salah Dimia, M., et al., *Collapse of concrete columns during and after the cooling phase of a fire.* Journal of Fire Protection Engineering, 2011. **21**(4): p. 245-263.
29. Franssen, J.-M. and V. Kodur, *Residual Load Bearing Capacity of Structures Exposed to Fire*, in *Structures 2001*. 2001. p. 1-12.
30. Kodur, V.K.R., et al., *Simplified approach for evaluating residual strength of fire-exposed reinforced concrete columns.* Materials and Structures, 2013. **46**(12): p. 2059-2075.
31. Kodur, V., D. Hibner, and A. Agrawal, *Residual response of reinforced concrete columns exposed to design fires.* Procedia Engineering, 2017. **210**: p. 574-581.
32. Chen, Y.-H., et al., *Experimental research on post-fire behaviour of reinforced concrete columns.* Fire safety journal, 2009. **44**(5): p. 741-748.
33. ISO, *ISO 834-1:1999. Fire-resistance tests — Elements of building construction — Part 1: General Requirements*. 1999, International Organization for Standardization: Geneva, Switzerland.
34. Demir, U., et al., *Post-fire Seismic Behavior of RC Columns Built with Sustainable Concrete.* Journal of Earthquake Engineering, 2021: p. 1-24.
35. Demir, U., et al., *Impact of time after fire on post-fire seismic behavior of RC columns.* Structures, 2020. **26**: p. 537-548.
36. Lie, T.T., *Structural Fire Protection*. Structural Fire Protection. 1992, New York: American Society of Civil Engineers.
37. Bisby, L.A., et al., *Strengthening fire-damaged concrete by confinement with fibre-reinforced polymer wraps.* Engineering Structures, 2011. **33**(12): p. 3381-3391.
38. Yaman S. S. Al-Kamaki and R. Al-Mahaidi, *Compressive strength of concrete damaged by elevated temperature and confined by CFRP fabrics*, in *Fourth Asia-Pacific Conference on FRP in Structures (APFIS 2013)*. 2013: Melbourne, Australia.
39. Yaqub, M. and C.G. Bailey, *Repair of fire damaged circular reinforced concrete columns with FRP composites.* Construction and Building Materials, 2011. **25**(1): p. 359-370.
40. Yaqub, M., C.G. Bailey, and P. Nedwell, *Axial capacity of post-heated square columns wrapped with FRP composites.* Cement and Concrete Composites, 2011. **33**(6): p. 694-701.
41. Yaqub, M. and C.G. Bailey, *Seismic performance of shear critical post-heated reinforced concrete square columns wrapped with FRP composites.* Construction and Building Materials, 2012. **34**: p. 457-469.
42. ISO, *ISO 834-1:1999 Fire-resistance tests - Elements of building construction - Part 1: General requirements*. 1999. p. 25.
43. REBA, *Decreto 47723 - Regulamento de Estruturas de Betao Armado*. 1967, Diário do Governo: Portugal.
44. NP-EN206, *Concrete - Specification, performance, production and conformity (Portuguese Version)*, IPQ, Editor. 2000, European Committee for Standardization: Portugal.
45. Maclean, J., *The Structural Response of Reinforced Concrete Columns During and After Exposure to Non-Uniform Heating and Cooling Regimes*. 2018, The University of Edinburgh: Edinburgh, Scotland, United Kingdom.
46. Maclean, J., L. Bisby, and C. Ibañez, *Effect of non-uniform heating and cooling on eccentrically loaded reinforced concrete columns*, in *SiF 2020 – The 11th International Conference on Structures in Fire*. 2020: Brisbane, Australia.
47. Bamonte, P. and F. Lo Monte, *Reinforced concrete columns exposed to standard fire: Comparison among different constitutive models for concrete at high temperature.* Fire Safety Journal, 2015. **71**: p. 310-323.

48. Gernay, T., *Effect of Transient Creep Strain Model on the Behavior of Concrete Columns Subjected to Heating and Cooling.* Fire Technology, 2012. **48**(2): p. 313-329.
49. Bamonte, P., et al., *Numerical investigation of the structural response of eccentrically loaded reinforced concrete columns exposed to non-uniform heating and cooling*, in *SiF 2020 – The 11th International Conference on Structures in Fire*. 2020: Brisbane, Australia.
50. Rodrigues, H., et al., *Experimental evaluation of rectangular reinforced concrete column behaviour under biaxial cyclic loading.* Earthquake Engineering & Structural Dynamics, 2013. **42**(2): p. 239-259.
51. Lucchini, A., et al., *Load Path Effect on the Response of Slender Lightly Reinforced Square RC Columns under Biaxial Bending.* Journal of Structural Engineering, 2022. **148**(3): p. 04021278.
52. Ingason, H. and U. Wickström, *Measuring incident radiant heat flux using the plate thermometer.* Fire Safety Journal, 2007. **42**(2): p. 161-166.
53. BSI, *BS EN 1994-1-2:2005. Eurocode 4: Design of composite steel and concrete structures — Part 1-2: General rules — Structural fire design*. 2005, British Standards International: London, United Kingdom.
54. BSI, *BS EN ISO 1504-3:2005 - Products and systems for the protection and repair of concrete structures. Definitions, requirements, quality control and evaluation of conformity - Part 3: Structural and non-structural repair*. 2006, British Standards International: London, United Kingdom.
55. CNR, *CNR-DT 200 R1/2013: Guide for the Design and Construction of Externally Bonded FRP Systems for Strengthening Existing Structures*. 2013, Consiglio Nazionale delle Ricerche: Rome, Italy.
56. Pohoryles, D.A., et al., *Experimental Comparison of Novel CFRP Retrofit Schemes for Realistic Full-Scale RC Beam-Column Joints.* Journal of Composites for Construction, 2018. **22**(5): p. 04018027.
57. ACI Committee 440, *ACI 440.2R-17 Guide for the Design and Construction of Externally Bonded FRP Systems for Strengthening Concrete Structures*. 2017, American Concrete Institute: Farmington Hills, MI, USA.
58. The Concrete Society, *Technical Report No. 55: Design guidance for strengthening concrete structures using fibre composite materials*. 2012: Camberley, United Kingdom.
59. Buchanan, A.H. and A.K. Abu, *Structural Design for Fire Safety*. 2nd ed. 2017, Chichester, UK: John Wiley & Sons Ltd.
60. Bisby, L.A., V.K.R. Kodur, and M.F. Green, *Fire Endurance of Fiber-Reinforced Polymer-Confined Concrete Columns.* ACI Structural Journal, 2005. **102**(6): p. 883-891.
61. Williams, B., et al., *Fire insulation schemes for FRP-strengthened concrete slabs.* Composites Part A: Applied Science and Manufacturing, 2006. **37**(8): p. 1151-1160.
62. Triantafyllidis, Z. and L.A. Bisby, *Fibre-reinforced intumescent fire protection coatings as a confining material for concrete columns.* Construction and Building Materials, 2020. **231**: p. 117085.
63. Park, Y.J. and H.S. Ang, *Seismic Damage Model for Reinforced Concrete.* ASCE - J Struct Eng, 1985. **111(4)**: p. 722-739.
64. CEN, *EN 1998-1:2004+A1 - Eurocode 8: Design of structures for earthquake resistance - Part 1: General rules, seismic actions and rules for buildings*. 2013, CEN: Brussels.
65. Melo, J., H. Varum, and T. Rossetto, *Experimental cyclic behaviour of RC columns with plain bars and proposal for Eurocode 8 formula improvement.* Engineering Structures, 2015. **88**: p. 22-36.